

## Heat Treatment and Microstructural Studies of LaNi-Type Battery Electrode Alloys

E.A. Ferreira, L.P. Barbosa, R.N. Faria

Energy and Nuclear Research Institute, IPEN/CNEN-SP  
Av. Prof. Lineu Prestes, 2242 - CEP 05508-000, São Paulo, Brazil

eafferreira@ipen.br, bluzinete22@gmail.com, rfaria@ipen.br

**Keywords:** La-Mg-Ni, hydrogen storage alloy, microstructures, properties.

**Abstract.** The effects of annealing on the microstructures and electrochemical characteristics of a  $\text{La}_{0.7}\text{Mg}_{0.3}\text{Al}_{0.3}\text{Mn}_{0.4}\text{Co}_{0.5}\text{Ni}_{3.8}$  hydrogen storage alloy have been studied. The heat treatment by vacuum annealing was carried out at 700 °C, 800 °C, 900 °C and 1000 °C. The microstructure and phase composition of the alloy have been investigated using inductively coupled plasma - atomic emission spectrometry (ICP-AES), scanning electron microscopy (SEM), energy dispersive X-ray analysis (EDX) and X-ray diffraction analysis (XRD). The battery anode was prepared using a mixture of the pulverized alloy with carbon black and polytetrafluoroethylene as a binder.

### Introduction

Hydrogen storage compounds have been studied extensively due to their potential to produce good negative electrode to nickel metal hydride batteries. Alloying additions to the base LaNi compound has been investigated as a means to improve their characteristics. The heat treatment at high temperature on the cast alloys has been employed as an additional way to increase the electrode properties [1-9]. In this study further investigation has been carried out on a  $\text{La}_{0.7}\text{Mg}_{0.3}\text{Al}_{0.3}\text{Mn}_{0.4}\text{Co}_{0.5}\text{Ni}_{3.8}$  alloy in the as-cast condition and after heat treatment at 700 °C, 800 °C, 900 °C and 1000 °C. The effects of high temperature annealing on the electric characteristics and microstructure of the alloy has been studied. Phase composition changes upon heat treatment have been investigated with energy dispersive X-rays (EDX) analysis and discharge capacity variations were studied by electrode cycling. A square-type cell with KOH electrolyte a nickel hydroxide cathode was used in the batteries testing.

### Experimental

Commercial copper mold alloy was investigated in this work. The chemical analysis carried out by inductively coupled plasma - atomic emission spectrometry (ICP-AES) of the cast alloy is given in Tab. 1.

**Table 1** – Chemical composition by ICP-AES of the  $\text{La}_{0.7}\text{Mg}_{0.3}\text{Al}_{0.3}\text{Mn}_{0.4}\text{Co}_{0.5}\text{Ni}_{3.8}$  alloy.

Alloy substitution composition (at. %)	Specified composition and analyzed composition (wt. %)					
	La	Mg	Al	Mn	Co	Ni
$\text{La}_{0.7}\text{Mg}_{0.3}\text{Al}_{0.3}\text{Mn}_{0.4}\text{Co}_{0.5}\text{Ni}_{3.8}$	25.12	1.88	2.09	5.68	7.61	57.62
	24.57	1.62	1.90	5.58	7.67	58.55

In order to prepare the battery the following procedure was adopted. Five grams of the cast  $\text{La}_{0.7}\text{Mg}_{0.3}\text{Al}_{0.3}\text{Mn}_{0.4}\text{Co}_{0.5}\text{Ni}_{3.8}$  alloy was crushed with a mortar and pestle in air, such that all the material passed through a < 44  $\mu\text{m}$  sieve. The powder (140 mg) was mixed with graphite and PTFE (140 mg) and pressed into a small electrode (approximately 2x2  $\text{cm}^2$ ; 1 mm thick). Separator and positive electrode  $\text{Ni}(\text{OH})_2$  were taken from a commercial battery. At the charge/discharge cycle tests, the charge was conducted using the current 14 mA during 5 hours and discharge at 7 mA until voltage reached -0.9 V. The Crystallographica Search-Match software (CSM) and PowderCell 2.3 software were used for X-ray pattern analyses.

## Results and discussion

The as-cast microstructures by SEM of the alloys with a typical grain structure are shown in Fig. 1. The chemical compositions of the phases, analyzed using EDX on a SEM in the as-cast alloy, are presented in Tab. 2. The  $\text{La}_{0.7}\text{Mg}_{0.3}\text{Al}_{0.3}\text{Mn}_{0.4}\text{Co}_{0.5}\text{Ni}_{3.8}$  alloy is composed mainly of the matrix phase and other phases in the grain boundaries. Rare earth (RE) content in the matrix phase was about 15 at. %. The lattice parameters and phase abundance of this cast alloy determined by X-ray diffraction are given in Tab. 3. The main phases of the alloy is  $\text{CaCu}_5$ -type hexagonal  $\text{LaNi}_5$  phase and  $\text{PuNi}_3$ -type rhombohedral  $(\text{La},\text{Mg})\text{Ni}_3$  phase. The annealed microstructures of the  $\text{La}_{0.7}\text{Mg}_{0.3}\text{Al}_{0.3}\text{Mn}_{0.4}\text{Co}_{0.5}\text{Ni}_{3.8}$  alloy are shown in Fig. 2.

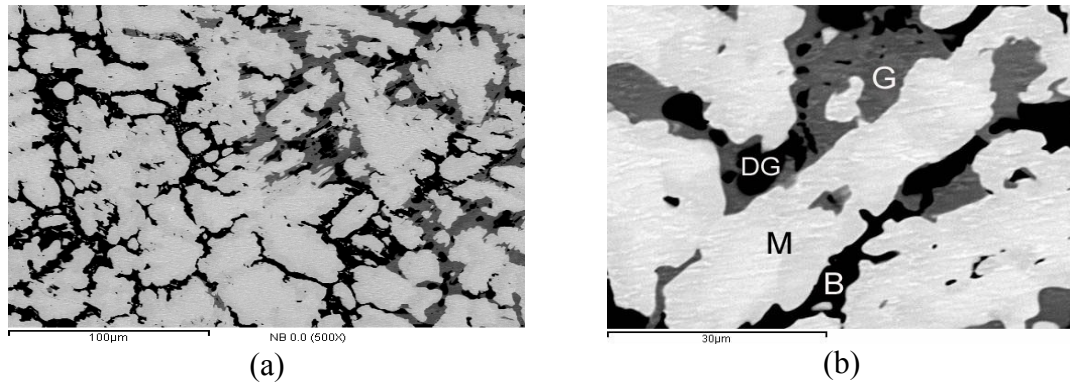


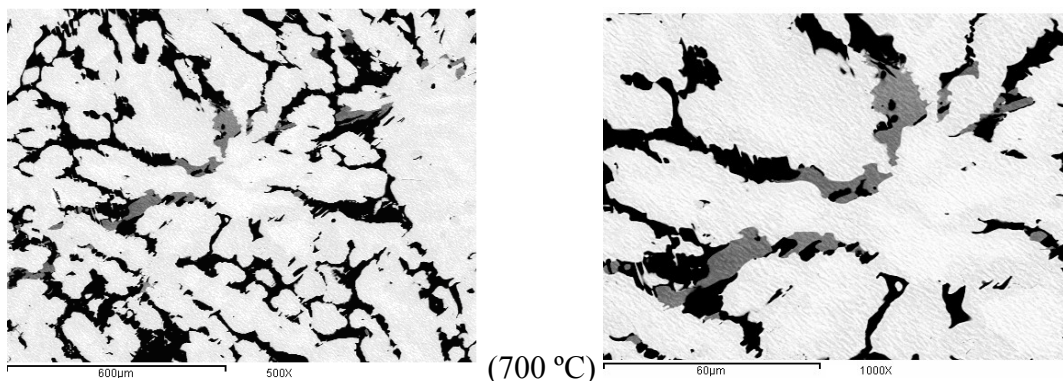
**Fig. 1** – Backscattered electron image of the as-cast microstructure of the  $\text{La}_{0.7}\text{Mg}_{0.3}\text{Al}_{0.3}\text{Mn}_{0.4}\text{Co}_{0.5}\text{Ni}_{3.8}$  as-cast alloy showing a general view (a) and details (b) of the matrix (M), the gray (G) the dark gray (DG) or black (B) phases.

**Table 2** – Chemical composition by EDX in the as-cast  $\text{La}_{0.7}\text{Mg}_{0.3}\text{Al}_{0.3}\text{Mn}_{0.4}\text{Co}_{0.5}\text{Ni}_{3.8}$  alloy.

Phase	Analyzed composition (wt %)					
	La	Mg	Al	Mn	Co	Ni
Matrix (M)	15.4±0.5	<1	4.5±0.2	2.5±0.5	7.9±0.6	69.5±0.9
Gray (G)	8.4±0.2	10.3±0.4	2.8±0.1	6.9±0.2	8.0±0.1	63.3±0.7
Dark (DG)	1.3±0.1	-	9.6±0.5	15.4±0.5	15.5±0.5	57.9±0.7

**Table 3** – Characteristics of structural parameters of main phases in the cast alloy.

Phase	Lattice parameter (Å)		Phase abundance (wt. %)
	a	c	
$\text{LaNi}_5$	5.067	4.036	62.1
$(\text{LaMg})\text{Ni}_3$	5.065	24.341	37.9



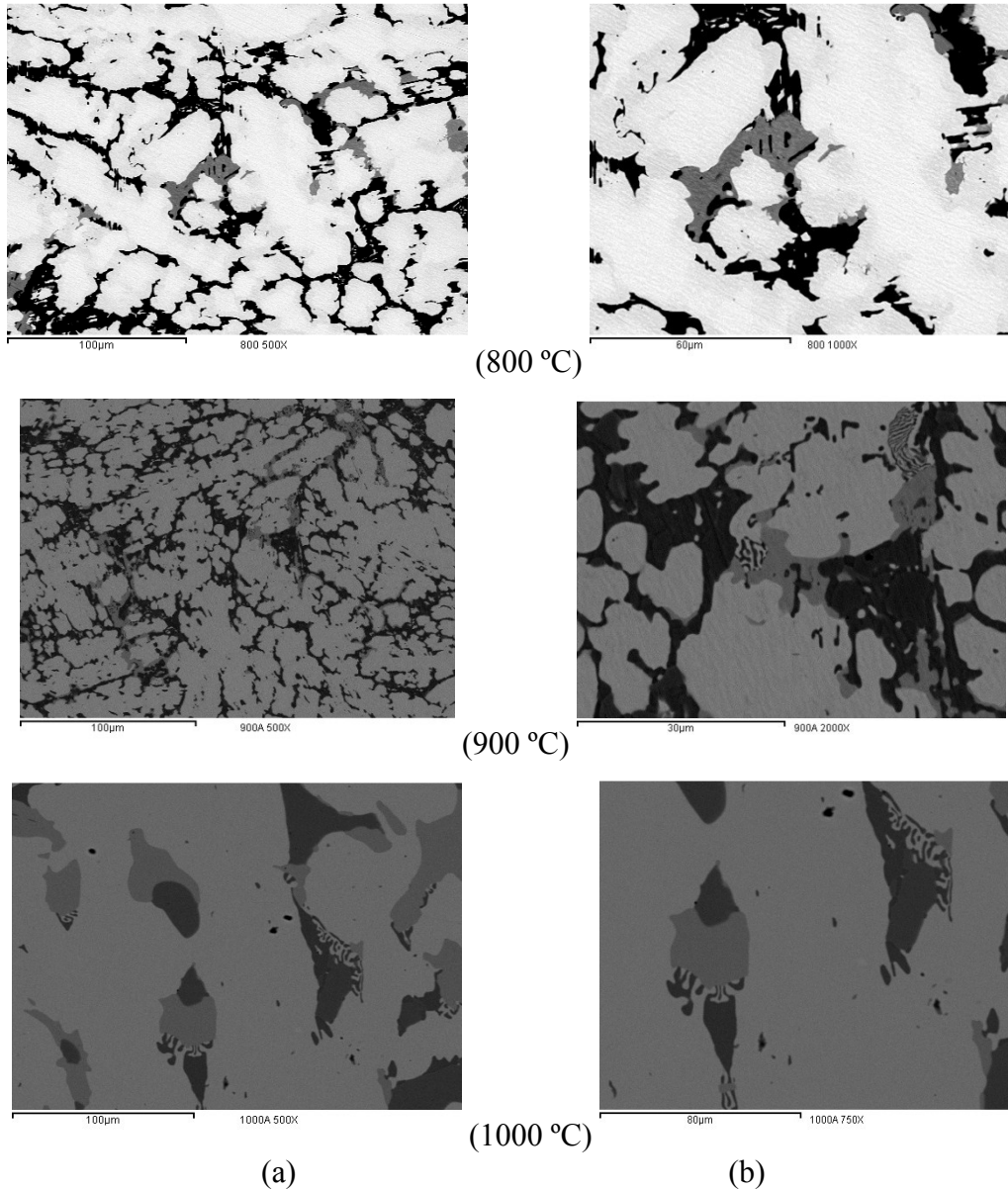


**Fig. 2** – Backscattered electron image of the as-cast microstructure of the  $\text{La}_{0.7}\text{Mg}_{0.3}\text{Al}_{0.3}\text{Mn}_{0.4}\text{Co}_{0.5}\text{Ni}_{3.8}$  annealed alloy showing a general view (a) and details (b).

The heating treatment changed the alloy microstructure by homogenization of the grain boundaries phases. The concentration of the gray phase was changed with heat treatment. There was slight increase in dark phase and decrease on the gray phase with increasing annealing temperature. The microstructure of the alloys showed some grain boundaries eutectic features on annealing at 900 °C and 1000 °C.

In the as-cast alloy, elements as Al, Mn and Co were found inside the matrix phase which showed a RE:(Al, Mn, Co, Ni) atomic ratio of approximately 5, indicating a 1:5-type phase. Magnesium was undetected inside the matrix phase for the as-cast condition. The gray phase showed a La content of approximately 8 at. %. The dark phase showed some variations on the composition and this has been attributed to the rapid cooling during casting on a water cooled copper mold. The chemical compositions of the phases, analyzed using EDX on the annealed alloys are presented in Tabs. 4-6.

After heat treatment the matrix phase showed a (La,Mg):(Al,Mn,Co,Ni) atomic ratio of about 5, confirming it to be a 1:5 phase. The amount of manganese on the matrix phase doubled on heat treatment of the as-cast alloy at 900 °C and 1000 °C. The other elements analyzed on this phase remained fairly constant within measurement error. Similar behavior was observed on the dark

phase upon heat treatment with no significant change on the amount of the various alloying elements. Conversely, the gray phase showed a significant variation on the composition of La, Mg Al and Mn upon heat treating at high temperature.

**Table 4** – Chemical composition of the matrix phase on  $\text{La}_{0.7}\text{Mg}_{0.3}\text{Al}_{0.3}\text{Mn}_{0.4}\text{Co}_{0.5}\text{Ni}_{3.8}$  alloy.

Temp. (°C)	Composition (at. %)						ratio (La,Mg):(Al,Mn,Co,Ni)
	La	Mg	Al	Mn	Co	Ni	
700	15.1 ± 0.1	<1	4.9 ± 0.3	4.4 ± 0.5	7.8 ± 0.8	67.5 ± 1.1	1 : 5
800	14.6 ± 0.6	<1	4.4 ± 0.3	4.7 ± 0.2	8.1 ± 0.5	67.3 ± 1.4	1 : 5
900	14.8 ± 0.1	1.2 ± 0.7	5.1 ± 0.3	5.0 ± 0.7	7.8 ± 0.5	65.9 ± 1.1	1 : 5
1000	15.4 ± 0.3	<1	4.3 ± 0.1	5.0 ± 0.4	7.9 ± 1.2	67.2 ± 1.3	1 : 5

**Table 5** – Chemical composition of the dark phase on  $\text{La}_{0.7}\text{Mg}_{0.3}\text{Al}_{0.3}\text{Mn}_{0.4}\text{Co}_{0.5}\text{Ni}_{3.8}$  alloy.

Temp. (°C)	Composition (at. %)						ratio (Al:Mn,Co,Ni)
	La	Mg	Al	Mn	Co	Ni	
700	1.9 ± 0.2	-	8.7 ± 0.5	15.4 ± 0.5	15.2 ± 0.5	58.6 ± 1.0	1 : 1.7-1.7-6.7
800	1.3 ± 0.1	1.0 ± 0.1	7.7 ± 0.3	18.1 ± 0.6	20.2 ± 0.6	51.5 ± 1.1	1 : 2.3-2.6-6.6
900	<1	1.1 ± 0.1	9.5 ± 0.4	16.6 ± 0.5	17.7 ± 0.5	54.2 ± 1.2	1 : 1.7-1.8-5.7
1000	1.2 ± 0.1	-	9.8 ± 0.5	15.9 ± 0.5	16.1 ± 0.5	56.8 ± 1.3	1 : 1.6-1.6-5.7

**Table 6** – Composition of the gray phase on  $\text{La}_{0.7}\text{Mg}_{0.3}\text{Al}_{0.3}\text{Mn}_{0.4}\text{Co}_{0.5}\text{Ni}_{3.8}$  alloy.

Temp. (°C)	Composition (at.%)						ratio (La,Mg):(Al,Mn,Co,Ni)
	La	Mg	Al	Mn	Co	Ni	
700	1.5 ± 0.1	17.8 ± 0.5	1.6 ± 0.2	11.2 ± 0.4	8.6 ± 0.1	59.1 ± 0.9	1 : 4.1
800	<1	21.4 ± 0.7	-	11.5 ± 0.5	8.1 ± 0.1	57.9 ± 1.0	1 : 3.6
900	3.6 ± 0.1	20.1 ± 0.5	1.7 ± 0.1	10.3 ± 0.5	8.2 ± 0.1	55.9 ± 1.0	1 : 3.2
1000	2.2 ± 0.1	20.0 ± 0.5	-	10.4 ± 0.5	8.0 ± 0.1	59.2 ± 1.1	1 : 3.5

The amount of La and Al in the gray phase was reduced considerably with heat treatment. The amount of magnesium in this phase doubled in most cases of the heat treated alloys. The manganese content also had an increase on treatment of the cast alloy, but not as substantial as the magnesium concentration. The (La,Mg):(Al,Mn,Co,Ni) atomic ratio of the analyzed gray phases varied somewhat upon heat treatment. X-ray diffraction patterns of  $\text{La}_{0.7}\text{Mg}_{0.3}\text{Al}_{0.3}\text{Mn}_{0.4}\text{Co}_{0.5}\text{Ni}_{3.8}$  alloy annealed at distinct temperatures are presented Fig. 3. The alloy annealed at these temperature are composed of the  $\text{LaNi}_5$  and  $(\text{La,Mg})\text{Ni}_3$  phases, as in the case of the as cast condition.

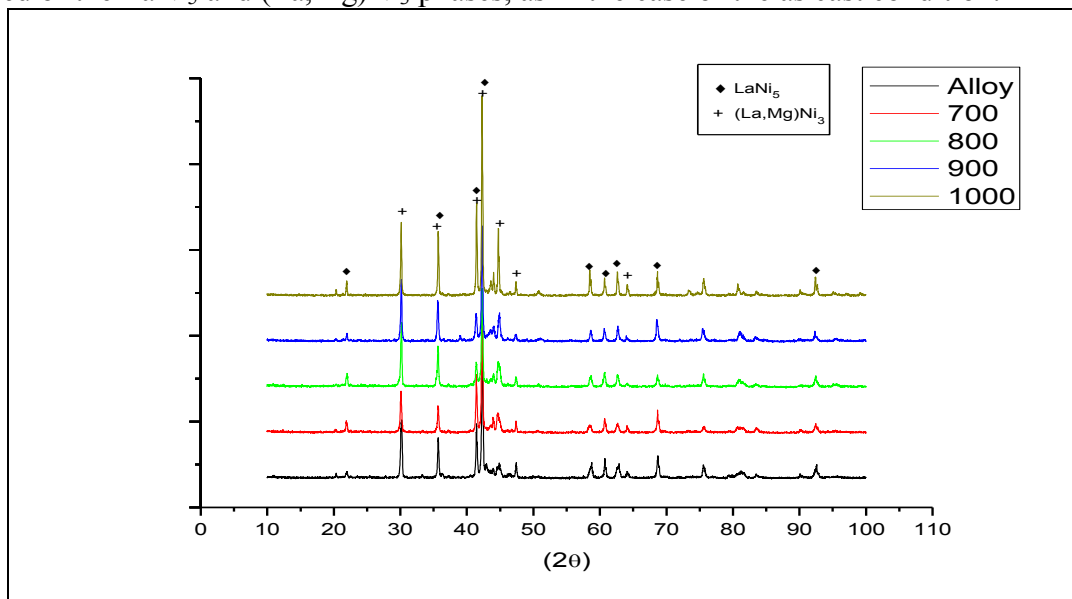


**Fig. 3** – X-ray diffraction patterns of the  $\text{La}_{0.7}\text{Mg}_{0.3}\text{Al}_{0.3}\text{Mn}_{0.4}\text{Co}_{0.5}\text{Ni}_{3.8}$  alloy.

The discharge capacities plotted versus cycle number of the batteries employing the various alloys conditions are shown in Fig. 4. The negative electrode produced with a  $\text{La}_{0.7}\text{Mg}_{0.3}\text{Al}_{0.3}\text{Mn}_{0.4}\text{Co}_{0.5}\text{Ni}_{3.8}$  alloy annealed at 800 °C exhibited the best performance. Annealing temperatures above 800 °C decreased considerably the electrode efficiency.

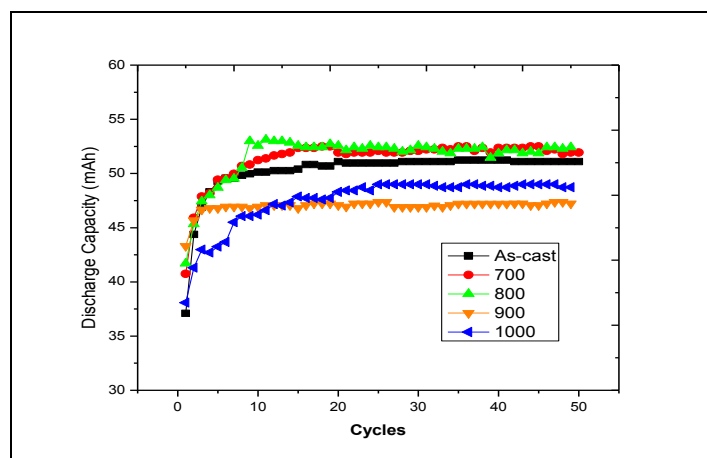


Fig. 4 – Cycle number dependence of the discharge capacity of the alloys.

## Conclusion

Annealing at high temperature produced considerable change on the cast microstructure of a  $\text{La}_{0.7}\text{Mg}_{0.3}\text{Al}_{0.3}\text{Mn}_{0.4}\text{Co}_{0.5}\text{Ni}_{3.8}$  ingot alloy. The high temperature heat treatment also modified the phase compositions present on the cast ingot alloy. The amount of manganese on the matrix and gray phases increased substantially on heat treatment of the as-cast alloy. Magnesium also had a concentration elevation on the gray phase and only small composition variations were observed on the dark phase upon annealing. The electrochemical performance and a maximum discharge capacity of negative electrodes were also affected by this heat treatment. High vacuum annealing at 800 °C proved to be the most effective to the battery efficiency.

## Acknowledgement

The authors wish to thank CAPES, CNPq, Euro Brazilian Windows (EBW II) and IPEN-CNEN/SP for the financial support and infrastructure made available to carry out this investigation.

## References

- [1] H. Nakamura, Y. Nakamura, S. Fujitani, I. Yonezu: *J. Alloys Compd.* Vol. 218 (2) (1995), p. 216.
- [2] W.K. Hu, D.M. Kim, S.W. Jeon, J.Y. Lee: *J. Alloys Compd.* Vol. 270 (1-2) (1998), p. 255.
- [3] J. Ma, H. Pan, C. Chen, Q. Wang: *Int. J. Hydrogen Energy* Vol. 27 (1) (2002), p. 57.
- [4] J.R. Ares, F. Cuevas, A. Percheron-Guégan: *Mater. Sci. Eng. B* Vol. 108 (1-2) (2004), p. 76.
- [5] Z.H. Ma, J.F. Qiu, L.X. Chen, Y.Q. Lei: *J. Power Sources* Vol. 125 (2) (2004), p. 267.
- [6] H. Pan, N. Chen, M. Gao, R. Li, Y. Lei, Q. Wang: *J. Alloys Compd.* Vol. 397 (1-2) (2005), p. 306.
- [7] F. Zhang, Y. Luo, J. Chen, R. Yan, L. Kang, J. Chen: *J. Power Sources* Vol. 150 (2005), p. 247.
- [8] D. Song, Y. Wang, Y. Liu, S. Han, L. Jiao, H. Yuan: *J. Rare Earths* Vol. 26 (3) (2008), p. 398.
- [9] Z. Zhou, Y. Song, S. Cui, C. Huang, W. Qian, C. Lin, Y. Zhang, Y. Lin: *J. Alloys Compd.* Vol. 501 (1) (2010), p. 47.